Separation Science and Technology
Publication details, including instructions for authors and subscription information:
http://www.informaworld.com/smpp/title~content=t713708471

N^{pro} Autoprotease Fusion Technology: Development, Characteristics, and Influential Factors

Astrid Dürauer[ab]; Karin Ahrer[ab]; Waltraud Kaar[ab]; Clemens Achmüller[bc]; Wolfgang Sprinzl[b]; Sabrina Mayer[b]; Bernhard Auer[bc]; Alois Jungbauer[ab]; Rainer Hahn[ab]
[a] Department of Biotechnology, University of Natural Resources and Applied Life Sciences Vienna, Vienna, Austria [b] Austrian Center of Industrial Biotechnology, Vienna, Austria [c] Institute of Biochemistry, University of Innsbruck, Innsbruck, Austria

Online publication date: 24 November 2010

To cite this Article Dürauer, Astrid , Ahrer, Karin , Kaar, Waltraud , Achmüller, Clemens , Sprinzl, Wolfgang , Mayer, Sabrina , Auer, Bernhard , Jungbauer, Alois and Hahn, Rainer(2010) 'N^{pro} Autoprotease Fusion Technology: Development, Characteristics, and Influential Factors', Separation Science and Technology, 45: 15, 2194 — 2209
To link to this Article: DOI: 10.1080/15228967.2010.507552
URL: http://dx.doi.org/10.1080/15228967.2010.507552

Separation Science and Technology, 45: 2194–2209, 2010

ISSN: 0149-6395 print/1520-5754 online
DOI: 10.1080/15228967.2010.507552

Taylor & Francis
Taylor & Francis Group

N^{pro} Autoprotease Fusion Technology: Development, Characteristics, and Influential Factors

Astrid Dürauer,[1,2] Karin Ahrer,[1,2] Waltraud Kaar,[1,2] Clemens Achmüller,[2,3] Wolfgang Sprinzl,[2] Sabrina Mayer,[2] Bernhard Auer,[2,3] Alois Jungbauer,[1,2] and Rainer Hahn[1,2]

[1]*Department of Biotechnology, University of Natural Resources and Applied Life Sciences Vienna, Vienna, Austria*
[2]*Austrian Center of Industrial Biotechnology, Vienna, Austria*
[3]*Institute of Biochemistry, University of Innsbruck, Innsbruck, Austria*

N^{pro} fusion technology enables the overexpression of peptides/proteins fused to an autoprotease and deposited as inclusion bodies in *E. coli*. Under kosmotropic conditions, the autoprotease cuts itself at the C terminus, releasing the target with an authentic N terminus. A tailor-made N^{pro} mutant, EDDIE, has overcome problems with low solubility and cleavage rate of wild-type N^{pro}. Codon optimization avoids truncation and prolongation of the fusion proteins. The examples presented demonstrate important factors (first amino acid of target, type of chaotrope) to optimize for raising the rate constant and yield of the autoproteolytic reaction, thus increasing protein production productivity up to 10-fold.

Keywords autoprotease; classical swine fever virus; cleavage; fusion protein; kinetics; refolding

INTRODUCTION

According to a recent technical market research report, the global market for protein therapeutics was worth $86.8 billion in 2007 and an estimated $95.2 billion in 2008, with a value expected to reach $160.1 billion in 2013. Although the drug development industry still focuses primarily on small molecules, in recent years, protein and peptide therapeutics comprise a significant percentage of the product line for most major pharmaceutical companies. Protein drugs have received enormous attention from these companies because of their combination of bioreactivity, specificity, safety, and overall success rate (1).

In response to this interest, a major demand of biotechnological processes has become the production of therapeutic proteins in large amounts with high homogeneity. Overexpression of proteins/peptides in *Escherichia coli* facilitates meeting this goal. Because of its well-known advantages of short reproduction time for high yields of targets under well-characterized physiological conditions, *E. coli* is second only to mammalian cell systems as the most widely used host for recombinant protein production. Nevertheless, drawbacks of this expression system include cell toxicity and degradation of overexpressed peptides/proteins. Several fusion-tag strategies have been applied to protect small peptides from degradation after translation, enhance expression of desired proteins, and ease downstream processing (2,3). A major concern for pharmaceutical applications associated with these approaches is the need for subsequent effective removal of tags and enzymes, which leads to additional processing steps. Most of these tags unquestionably improved production and purification processes; however, incomplete cleavage by methionine aminopeptidase (4) may lead to intolerable microheterogeneity of the product and even change the product's functionality and stability (5,6). Thus, N- or C-terminal fusion tags must be removed, either enzymatically with specific proteases (7) or by the use of intein self-cleavage systems (8). Inteins as fusion partners in recombinant protein expression have an exceptional position, since they provide an inducible self cleavage system and therefore do not require further enzymes for tag cleavage. Their natural function is protein splicing, a post-translational process for the excision of intervening sequences that interrupt the coding sequences of a certain gene (9). Most inteins have an N-terminal cysteine or serine, a C-terminal asparagine and are inserted into the host protein before a nucleophilic amino acid (cysteine, serine or threonine) (10–12). Their benefit in biotechnological

Received 24 October 2009; accepted 7 July 2010.

Current address for authors Karin Ahrer and Waltraud Kaar: Octapharma Pharmazeutika, Oberlaaer Straße 235, 1100 Vienna, Austria.

Address correspondence to Rainer Hahn, Department of Biotechnology, University of Natural Resources and Applied Life Sciences Vienna, Muthgasse 18, 1190 Vienna, Austria. Fax: +0043 1 3697615. E-mail: Rainer.Hahn@boku.ac.at

processes has been recognized since not only splicing but also coupling reactions, protein cyclization, polymerization, and site specific cleavage could be accomplished by modifying the splicing element with respect to its N- or C-terminal amino acids and adjusting the conditions favoring these side reactions in protein splicing. The first intein mediated protein expression and purification systems have been introduced in 1997 (13). By further improvement a versatile expression set, the IMPACT^{TM} (Intein Mediated Purification with an Affinity Chitin-binding Tag) system from New England Biolabs, was established. It allows the production of proteins with an N-terminal amino acid other than methionine by thiol induced cleavage, cleavage by pH or temperature shift, the production of cyclic polypeptides, and the ligation of expression products. It features a chitin binding tag which enables purification and cleavage in a single chromatographic step. Thiol cleavage is performed at highly reducing conditions which may affect disulfid bondage of the target protein and produces a small intein fragment when the intein is fused N-terminally. pH or temperature induced cleavage leads to target proteins with an N-terminal cysteine. Despite its distinct advantages, intein fusion technology is still limited to laboratory scale due to the high cost of affinity matrices (14). The introduction of N^{pro} fusion technology has largely helped to overcome constraints affecting the applicability of fusion strategies for industrial and particularly for pharmaceutical applications. This system is based on the autoprotease N^{pro} derived from classical swine fever virus or its mutant EDDIE as an N-terminal self-cleavable fusion tag (15). Table 1 shows the amino acid sequences

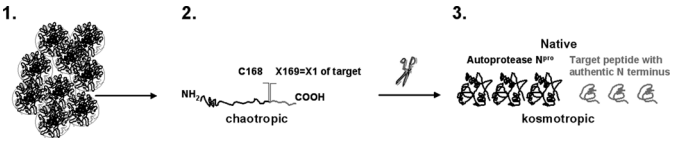

FIG. 1. Schematic Overview of the Autoprotease Fusion Concept: 1. N^{pro} fusion proteins are expressed in IBs in inactive form. 2. Dissolution of IBs with a high concentration of chaotropic reagents. 3. Refolding under kosmotropic conditions leads to autoproteolytic cleavage and release of the native target protein with an authentic N terminus.

of N^{pro} wildtype and mutant EDDIE in comparison. N^{pro} exhibits the unique feature of autoproteolytic activity at its own C terminus (16,17) and releases the fused target protein with a distinct N terminus upon renaturation. Figure 1 shows a schematic overview of N^{pro} fusion technology. The N^{pro} expression system represents a widely applicable tool for high-level expression of recombinant peptides and proteins without the need for chemical or enzymatic tag removal. In particular, toxic and difficult-to-express proteins have been expressed at high titers. Furthermore, authentic N termini have been produced for all investigated fusion partners (15).

N^{pro} fusions, like most heterologous proteins overexpressed in *E. coli*, are deposited as insoluble aggregates, also referred to as refractile bodies or inclusion bodies (IBs). Because of their high density, IB isolation can simply be carried out by differential centrifugation after cell disruption (18). Subsequent solubilization is accomplished with chaotropic agents such as urea or guanidine chloride

TABLE 1
Amino acid sequences of N^{pro} and mutant EDDIE; exchanged amino acids are in bold

N^{pro}

```
     1         11         21         31         41         51
     |         |          |          |          |          |
   1 MELNHFELLY KTSKQKPVGV EEPVYDTAGR PLFGNPSEVH PQSTLKLPHD RGRGDIRTTL  60
  61 RDLPRKGDCR SGNHLGPVSG IYIKPGPVYY QDYTGPVYHR APLEFFDEAQ FCEVTKRIGR 120
 121 VTGSDGKLYH IYVCVDGCIL LKLAKRGTPR TLKWIRNFTN CPLWVTSC
```

EDDIE

```
     1         11         21         31         41         51
     |         |          |          |          |          |
   1 MELNHFELLY KTSKQKPVGV EEPVYDTAGR PLFGNPSEVH PQSTLKLPHD RGEDDIETTL  60
  61 RDLPRKGDCR SGNHLGPVSG IYIKPGPVYY QDYTGPVYHR APLEFFDETQ FEETTKRIGR 120
 121 VTGSDGKLYH IYVEVDGEIL LKQAKRGTPR TLKWTRNTTN CPLWVTSC
```

at a high concentration. Detergents, organic solvents, or aqueous buffers at an alkaline pH may also be used (19).

Efficient solubilization is the first crucial step during IB processing, and dissolving conditions are usually empirically established. Recently, the current authors described a methodology for rapid screening of solubilization conditions and evaluation of dissolution kinetics at the microliter scale. Increased protein in solution over time was directly related to decreased turbidity measured by absorbance at 600 nm. This approach was the first available HTS for determination of IB dissolution kinetics. Of course, this methodology is not limited to screening of optimal buffer conditions for solubilization but can be applied for studying other parameters involved in IB solubility, such as pI of the protein, fermentation conditions, initial protein concentration, and more (20). This approach enabled the determination of dissolution kinetics that allowed a quantitative estimation of the solubilization process. This review presents applications of this screening system with N^{pro} fusion proteins.

To reconstitute their biological activity, unfolded proteins must be converted into their native three-dimensional structures. Thus, a major challenge for downstream processing of proteins deposited in IBs is refolding at high yield to take advantage of the high productivity of *E. coli* expression systems. A major loss of product during the production processes occurs in the refolding step, and yields close to 100% are rarely achieved. The yield of refolding is specific for the individual protein, and for each protein, proper conditions must be defined to ensure maximal yield.

Protein refolding is a concentration-sensitive process because side reactions, particularly misfolding and aggregation, occur simultaneously and very often with a higher reaction order (21). Refolding and aggregation reactions have been described by a differential mass balance assuming that the back reaction from folded or aggregated protein to unfolded protein is negligible and that formation of intermediates is infinitely fast. Kiefhaber and co-workers (22) have developed a model accounting for the case of aggregation occurring as a second-order reaction. Their solution includes the concentration of native protein, and the overall yield $Y(t)$ can be expressed as:

$$Y(t) = \frac{k_1}{U_0 K_2} \ln\left[1 + \frac{U_0 K_2}{k_1}(1 - e_1^{-k} t)\right] \qquad (1)$$

where U_0 [mol/L] is the initial concentration of the denatured protein, k_1 [s^{-1}] is the rate constant of folding, K_2 [$M^{-1}s^{-1}$] is the apparent rate constant of aggregation combining aggregation number N and rate constant of aggregation k_2, and t [s] is the time. For characterization of refolding and cleavage of N^{pro} fusions, the kinetics of this process have been calculated after determining either the amount of cleaved autoprotease or target protein/peptide compared to the corresponding amount available in the fusion protein. Based on these experimental data, Kaar et al. (23) showed that the kinetics of N^{pro}-protein fusion followed this reaction while that of N^{pro}-peptide fusions did not. A novel reaction scheme has been proposed by them assuming a side reaction other than aggregation that follows a first-order kinetics. Thus, the overall yield becomes independent of protein concentration (23).

The current work moves from the basics of N^{pro} fusion technology to improvements in the system from wild-type autoproteases with low solubility and cleavage yield to the tailor-made mutant EDDIE, which has the same specific autoproteolytic activity but with highly improved solubility and cleavage yield (15). Second, the study addresses the necessity of codon optimization for this system, showing one-dimensional (1D) and two-dimensional (2D) electrophoresis and mass spectral analysis of EDDIE fusions. Further, interesting characteristics of N^{pro} fusion technology are a focus, with a comparison of the N^{pro}-protein fusion 6H-EDDIE-sGFPmut3.1 to an N^{pro}-peptide fusion, EDDIE-pep6His. pep6His is a short peptide of 16 amino acids consisting of 10 randomly chosen amino acids and a C-terminal polyhistidine tag. These two model systems are used to examine the differences in refolding and cleavage kinetics and related to the established models of Kiefhaber et al. and Kaar et al. (22,23). Furthermore, dissolution kinetics are described for IBs containing 6H-EDDIE-GFPmut3.1 or EDDIE-pep6His, comparing urea and guanidinium chloride at different concentrations, and directly combined with refolding and cleavage kinetics. This manuscript will summarize some recently published papers on N^{pro} fusion technology combined with new data comparing expression and processing of peptides to proteins. It is an overview of the development and essential findings concerning this versatile tool showing the practical relevance regarding productivity and further perspectives of this technology.

MATERIALS AND METHODS

Chemicals

Dimethylformamide (DMF), CyDye™ DIGE Fluor Cy2 minimal dye, CyDye™ DIGE Fluor Cy3 minimal dye, CyDye™ DIGE Fluor Cy5 minimal dye, Immobiline™ DryStrip pH 3–10 NL 18 cm, ImmobilineTM DryStrip pH 6.2–7.5 18 cm, acrylamide PAGE 40% solution, IPG buffer 3–10 NL, IPG buffer 6.2–7.5, TEMED, ammonium persulfate, and ECF™ substrate for alkaline phosphatase were obtained from GE Healthcare (Uppsala, Sweden). Piperazine diacrylamide and PrecisionPlusProteinTM Standards All Blue were purchased from BioRad (Hercules, CA, USA). NuPAGE® LDS Sample Buffer,

NuPage-Bis-Tris 4–12% gradient gels, and SeeBlue® Plus2 prestained standard were from Invitrogen (Carlsbad, CA, USA). All other reagents were of analytical grade from Merck (Darmstadt, Germany) and Sigma (Saint Louis, MO, USA), respectively, if not otherwise indicated.

Recombinant Protein Expression and IB Isolation

The recombinant proteins N^{pro}-pep6His, EDDIE-pep6His, 6H-N^{pro}-sGFPmut3.1, and 6H-EDDIE-sGFPmut3.1 were overexpressed in *E. coli* BL21 with a pET30a plasmid (Novagen, Madison, WI, USA) containing the corresponding coding gene (15). *E. coli* fed-batch cultivation was performed with a semi-synthetic medium on a 5-L scale according to Clementschitsch et al. (24). Pep6His is a short sixteen amino acid peptide (pep6His) consisting of 10 randomly chosen amino acids and a C-terminal polyhistidine tag. After harvesting and washing with 0.9% NaCl, the wet cell paste was resuspended by sonication using an Ultra-Turrax T25 homogenizer (IKA® Werke, Staufen, Germany) in 50 mM Tris/HCl, pH 8.0, to approximately 5% dry matter. The slurry was passed three times through an APV 2000 lab homogenizer (Invensys, Albertslund, Denmark) at a pressure of 800 to 900 bar. IBs were separated by low-speed centrifugation for 30 minutes at $7500 \times g$. The resulting pellet was washed twice with 1% (v/v) Triton X-100. After two more washing steps (1 M NaCl, H_2O), each followed by a homogenizer passage, the IBs were resuspended in H_2O at a concentration of between 5% and 10% dry matter and stored at −20°C. Samples were drawn after each step and examined with SDS-PAGE.

Self-Interaction Assays

Cellulose-bound peptide libraries were semi-automatically prepared according to the method first published by Frank et al. slightly modified as described by Pflegerl et al. and Dürauer et al. (20,25,26) Briefly, peptides were immobilized C terminally on cellulose membranes via double β-alanine anchors, and a conventional 9-fluorenylmethoxycarbonyl technique was used for further peptide assembly. All amino acids as well as PyBOP® were purchased from Novabiochem (Läuflingen, Switzerland). After N-terminal acetylation of the last amino acid and cleavage of side-chain protection groups by treatment with trifluoroacetic acid (TFA), membranes were used immediately or dried and stored at −20°C. Membranes used previously were conditioned with 20% (v/v) methanol for at least 2 hours.

Wild-type N^{pro} and EDDIE were biotinylated in phosphate buffered saline, pH 7.3, containing 4 M urea to retain samples in their denatured state, at a concentration of around 0.5–3 mg/mL. Succinimidyl 6-(biotinamido)-hexanoate (Sigma, Vienna, Austria) was dissolved in dry DMF at a concentration of 20 mmol. This stock solution was added to the sample solution to obtain a 5-fold molar excess. The reaction mixture was incubated for two hours at room temperature or alternatively overnight at 4°C. Reaction byproducts were removed by gel filtration using PD10 columns (GE Healthcare, Uppsala, Sweden). For self-interaction assays, spot membranes covering the entire sequence of N^{pro} wild-type and EDDIE, 168 amino acids as 12mer peptides with an overlap of one amino acid, were washed three times with incubation buffer and blocked with a 3% bovine serum albumin solution overnight. N^{pro} and biotin-labeled EDDIE were diluted to a concentration in the range of 0.1–5 μg/mL in incubation buffer (100 mM phosphate, 2 or 4 M urea, 150 mM NaCl, 0.1% Tween 20 at pH 7.3) containing 1% BSA. After a 1-hour incubation, the membranes were washed thrice with incubation buffer and once with incubation buffer without urea. Afterwards the membranes were reacted with a streptavidin-horse radish peroxidase conjugate (Sigma, Vienna, Austria), diluted 1: 2000 into phosphate buffer containing 0.8 M NaCl, for 15 minutes. Subsequent detection was carried out with the Super Signal® West Pico chemiluminescence detection system (Pierce, Rockford, IL, USA) and LumiImager™ (Roche Diagnostics, Mannheim, Germany). Buffer components were all purchased from Merck (Vienna, Austria).

SDS-PAGE

SDS-PAGE was carried out with NuPAGE®-Bis-Tris 4–12% gradient gels in the Xcell IITM Mini-Cell (Invitrogen, Carlsbad, CA, USA) system using a MES-running buffer containing 50 mM MES, 50 mM Tris Base, 0.1% SDS, and 0.03% EDTA at a constant voltage of 200 V. For reducing samples, samples were cooked in NuPAGE® LDS Sample Buffer and 10% v/v of 2 M dithiothreitol (DTT) for 10 minutes at 100°C. Protein bands were detected by Colloidal Blue Staining (Invitrogen, Carlsbad, CA, USA). SeeBlue®Plus2 prestained standard (Invitrogen, Carlsbad, CA, USA) was used as the molecular mass standard.

2-dimensional Electrophoresis (2-DE)

The various IBs were separated by isoelectric focusing (IEF) in Immobiline Dry Strips, pH 3–10 NL, 18 cm. Strips were rehydrated overnight in an appropriate reswelling tray in a solution containing 8 M urea, 2% CHAPS, 20 mM DTT, 0.5% IPG buffer, and traces of bromophenol blue. IEF was performed on a Multiphor II electrophoresis unit (GE Healthcare, Uppsala, Sweden) in combination with an EPS 3501 XL power supply (GE Healthcare, Uppsala, Sweden) at 20°C. Samples applied on IPG strips contained 2% of IPG buffer. The protein amount applied on the IPG strips varied from 15–150 μgIEF was terminated when more than 50,000 kVh at step 7 (Table 2) were achieved. After IEF, the strips were equilibrated for SDS-PAGE by incubation for two intervals of 10 minutes in 8 M urea, 2% SDS, 30% glycerol, and 50 mM Tris/HCl,

TABLE 2
Running conditions for 3–10 NL Immobiline drystrips on a multiphor II electrophoresis system. Running conditions: Temperature 20°C, current 50 μA/strip, power 5 W total

	Voltage [V]	Time [h:min]
Step 1 (linear)	100	00:30
Step 2 (gradient)	300	00:30
Step 3 (linear)	300	00:30
Step 4 (gradient)	500	00:30
Step 5 (linear)	500	00:30
Step 6 (gradient)	2,000	02:30
Step 7 (linear)	2,000	03:00
Step 8 (gradient)	8,000	24:00

pH 6.8, for 10 minutes. DTT (2%) was added to the first equilibration, and iodoacetamide (2.5%) was added to the second equilibration solution. The strips were transferred to 1-mm–thick 12.5% AA SDS-PAGE gels. Vertical SDS electrophoresis was performed on an ETTAN DALT system (GE Healthcare, Uppsala, Sweden) with a SDS gel running buffer prepared according to Laemmli. Afterwards, 2D PAGE gels containing CyDye-labeled samples were immediately scanned on a Typhoon 9400 Variable Mode Imager. Labeling with minimal CyDyes was done according to the manufacturer's protocol. Image analysis, including spot quantification and matching between gels, was achieved with the DeCyder software (GE Healthcare, Uppsala, Sweden). Table 2 summarizes the running conditions for 3–10 NL Immobiline DryStrips on a Multiphor II electrophoresis system.

Mass Spectrometric (MS) Analysis

MS was performed on a Q-TOF Ultima Global (Waters Micromass, UK). The particular sample was diluted in 50% acetonitrile containing 0.1% formic acid to give a final concentration of ~20–25 pmol/μL. Samples were introduced offline to ESI Q-TOF MS. The mass spectrometer had been previously tuned with [Glu1]-fibrinopeptide B to give the highest possible sensitivity and a resolution of ca. 10,000 (FWHM). Mass tuning of the TOF analyzer was done in the tandem MS mode again using [Glu1]-fibrinopeptide B. For data acquisition, MassLynx 4.0 Software (Waters Micromass, Milford, MA) was used. For determination of protein masses from the acquired MS data, deconvolution was performed using the MaxEnt1 function of MassLynx software.

Determination of Dissolution Kinetics

Prior to the experiments, IBs were lyophilized and stored at 4°C, and adequate quantities of these dried powders were measured for each experiment. If not mentioned otherwise, the experiments used 20 mg/mL lyophilized IBs as the starting concentration. IBs were suspended in 1 mL of corresponding buffer, and four 180-μL aliquots along with two aliquots of blank buffer were transferred to a microtiter plate (transparent flat bottom, low absorbance; Greiner, Germany). Absorbance at 600 nm was immediately measured on a multifunctional microtiter plate reader (GENiosPro, TECAN, Männedorf, Switzerland), calculating an average value of 10 reads per well with 5 seconds of shaking prior to each measurement. Afterwards, the microtiter plate was placed on an orbital microtiter plate shaker (Thermomixer comfort MTP, eppendorf, Hamburg, Germany) at 550 rpm at 21°C. The same amount of IBs was suspended in 1 mL of water, and four 180-μL aliquots were transferred to the same microtiter plate and measured in parallel. More samples were added at defined starting points, and the absorbance at 600 nm was determined for an entire plate at specific time points over 4 hours. After 4 hours, dissolution in all wells was stopped by centrifugation at 13,200 rpm at 21°C for 5 minutes (Centrifuge 5415 R, eppendorf, Hamburg, Germany). All supernatants were diluted 1:41 in 8 M urea in microtiter plates, and absorbance at 280 nm was determined using a multifunctional microtiter plate reader (GENios Pro, TECAN, Männedorf, Switzerland).

For calculation of protein concentration in solution, a calibration curve was established by diluting one supernatant (preferably the sample with the highest expected protein concentration) and determining the absorbance at 280 nm in a quartz cuvette using a UV-visible spectrophotometer (CARY 50 Bio, UV-Visible Spectrometer, VARIAN Inc., Palo Alto, CA). Prior to further calculation, all values were reduced by corresponding buffer blank values. For conversion of the decrease in turbidity into an increase in protein in solution, the absorbance curve determined at 600 nm was mirrored. For calculating the curve as protein concentration in solution, the highest value after mirroring was normalized with the protein concentration in the corresponding well. Protein concentration in solution was calculated as the percentage of total protein present in the well. Calculated rate constants for dissolution kinetics are abbreviated with k_{sol}.

For the current work, lyophilized IBs were suspended in dissolution buffer containing different concentrations of urea or guanidinium hydrochloride (GuHCl) with or without the reducing agent monothioglycerol (MTG). Aliquots of these suspensions together with one aqueous suspension of the corresponding IBs were transferred to a 96-well microtiter plate, and turbidity was consecutively measured at 600 nm in all wells over 4 hours. The final protein concentration in each well was determined at 280 nm and calculated using an external calibration curve. Then dissolution kinetics were calculated as described earlier (20). Increasing concentrations of urea (4, 6, 8, and 10 M) were

compared to increasing concentrations of GuHCl (2, 3, 4, and 5 M), all with and without 100 mM MTG as an example illustrating the influence of buffer components on dissolution.

Protein Refolding

To extract the IB proteins, the IBs (isolated as described above) were suspended at a ratio of 1:5 into 10 M urea, 50 mM Tris/HCl, pH 7.3, supplemented with 50 mM DTT, followed by centrifugation and consecutive filtration through 0.4-μm and 0.22-μm syringe filters (Millipore, Billerica, MA, USA) to remove insoluble components.

Different concentrations of each protein were prepared by rapid dilution into the optimized refolding buffer (1 M Tris/HCl, 0.25 M sucrose, 2 mM EDTA, 20 mM MTG, pH 7.3) to a final volume of 10 mL using a high stirring speed. A homogeneous sample preparation was assured by stirring at 100 rpm for 30 seconds in a 20-mL beaker using a laboratory stirrer. Subsequently, refolding samples were incubated at 18°C without stirring. Immediately after dilution of protein into the refolding buffer, an aliquot of the refolding sample was transferred to an HPLC vial, and consecutive RP-HPLC analyses were performed at discrete time intervals from the same vial to follow the time course of refolding. In the case of sGFPmut3.1 fusion proteins, aliquots were transferred into black Costar® microplates (Corning Costar, Bodenheim, Germany), and fluorescence measurements were performed on a SpectraMax GeminiXS (Molecular Devices, Sunnyvale, CA, USA) at distinct time points, at which emission was recorded at 530 nm with a cutoff of 520 nm using an excitation wavelength of 488 nm. Calibration of relative fluorescence units was performed with sGFPmut3.1 (purified from fermentation of native sGFPmut3.1 laboratory preparation) over the range of 0.2 to 40 μg/mL. Fitting of data sets was accomplished with Table Curve 2D v5.0 and Table Curve 3D v2.0 (SPSS, Erkrath, Germany).

Reversed-Phase HPLC for Refolding and Cleavage Kinetics

Protein analyses by reversed-phase (RP)-HPLC were performed on an Agilent 1100 series chromatography system (Waldbronn, Germany) with a Jupiter™ C-4 column (2 × 150 mm, 5 μ, 300 Å) (Phenomenex, Torrance, CA, USA) equipped with an additional SecurityGuard™-cartridge. A buffer system of 0.1% (v/v) TFA, 5% (v/v) acetonitrile (AcCN) (LiChrosolv, Merck, Darmstadt, Germany) in water as buffer A and 0.1% (v/v) TFA in AcCN as buffer B was used. IB protein samples were prepared by dilution of at least 1:5 with 50 mM Tris/HCl, 6 M GuHCl, and 50 mM DTT, pH 7.3. Refolding samples were directly injected. Elution was performed with gradients differing in steepness depending on the cleavage products to be analyzed. Detection proceeded at two wavelengths, 214 nm and 280 nm, to allow distinction between proteins and buffer components. Calibration curves for EDDIE-pep6His and pep6His were established to allow quantification of IB protein and cleavage products. As reference standards, pep6His was produced by solid-phase peptide synthesis (26).

RESULTS AND DISCUSSION

The idea behind this autoprotease fusion technology was, on the one hand, to establish a prokaryotic expression system to overcome the current limitations of *E. coli* expression, including degradation of small proteins and peptides and the cytotoxic effects of targets. On the other hand, a focus was easing downstream processing requirements and avoiding additional purification steps for removal of fusion tags. As shown by Achmüller et al. (15), this goal had been achieved by expressing the target proteins and peptides fused to the autoprotease N^{pro} from classical swine fever virus. These fusion proteins are mostly deposited as IBs, which must be dissolved under harsh conditions with a high chaotrope concentration. By switching from chaotropic to kosmotropic conditions, e.g., by diluting the IB solutions with an adequate buffer, the autoprotease will cleave itself at its C terminus and release the target protein/peptide with an authentic N terminus. Since the intein self-cleavage technology offers similar features as the currently discussed system, we include a comparison of these two fusion technologies based on our experience and results reported in the literature (Table 3).

Expression of N^{pro} Fusion Proteins

A prominent feature of N^{pro} fusion technology is the very high expression level of recombinant proteins. Using high cell density fermentation, volumetric yields up to 12.5 g/L of fusion protein can be obtained, with 95% accumulated as IBs. Several examples with difficult-to-express proteins have proven the excellent features of this system. For instance, the expression yield for recombinant human monocyte chemoattractant protein could be increased approximately 10-fold (15). To our knowledge, the keratin-associated protein 10–4, also known as JAC, cannot be expressed by any other recombinant technology except N^{pro} fusion technology because of its high toxicity (27). For intein-self cleavage technology yields of protein production of 7 to 50 mg/L are reported, which is far below the expression level of the N^{pro} fusion system and can be partially explained by the inherent instability of the intein system (28). The intein-self cleavage system does not prefer soluble form or inclusion bodies, expressed proteins are available in both forms mostly depending on the properties of the target proteins (29,30).

It is also worth mentioning that so far, all proteins expressed by N^{pro} fusion technology for formation of an authentic N terminus could be confirmed by ESI Q-ToF

TABLE 3
Comparison of N^{pro} to intein-based fusion technology

	N^{pro} autoprotease system	Intein-based cleavage
Yield of protein production	up to 12.5 g/L (15)	7 to 50 mg/L (28)
Fusion protein as	Inclusion bodies (15)	Soluble form/Inclusion bodies (29,30)
Induction of cleavage	By switch from chaotropic to kosmotropic conditions (15,23,38)	By addition of thiols or pH/temperature shift (11,14)
Cleavage condition	1 M Tris/HCl, 0.25 M sucrose, 2 mM EDTA, 20 mM MTG, pH 7.3 (23)	0.9 M GuHCl, 0.1 M Tris/HCl, 2 M EDTA, 1 mM L-Cysteine, 1 mM L-Cystine (29)
Terminus of target protein and influence of target terminus	Authentic N terminus (15). All residues possible except for Pro (no cleavage) Gly, Met, Ala - most efficient (>88%) (15)	Authentic N terminus (29) IMPACT-CN: C terminal fusions: Met/Tyr /Phe preferred; Asp, Pro, Gly, Ala decrease efficiency N terminal fusions: Cys-Arg,Gly-Arg, Ser-Arg peferred, Pro no cleavage (14) Sce VMA (thiol induced cleavage): N terminus of target: all possible except for Ser, Cys, Pro possible; Met, Ala, Gln–most efficient (>95%) (8) For pH/temperature shift: N–terminus of target: Cys
Cleavage rate in vitro	20–90% (15)	20–90% (14)
Removal of tag after cleavage	Autoprotease removal by acidic precipitation at pH 5.0	Intein removal by affinity chromatography

MS analysis (15). Studies investigating the influence of the N terminal residue of the target protein on cleavage rate of the N^{pro} fusion system showed, that in vitro cleavage takes place in the presence of all amino acids except for proline, though the rates differ from 42 to 88% in vitro cleavage rate (15). Within the last two decades a big effort has been made to adapt the intein self-cleavage system for the production of a wide range of target proteins. Nowadays, systems for C terminal and N terminal fusion of target, thiol induced cleavage and cleavage induced by pH/temperature shift are available even in combination. Hence the limitation to specific N or C terminal residues of the target has been widely overcome. It is the same as for the N^{pro} fusion system, only an N-terminal proline fully prohibits cleavage. A summary of possible target termini and their influence on the cleavage rate is shown in Table 3.

Comparing Wild-Type Autoprotease N^{pro} to Mutant EDDIE

Initial use of wild-type autoprotease N^{pro} led to great difficulties regarding solubility, which were overcome by engineering a mutant called EDDIE. By exchange of 11 amino acids, the theoretical pI and the aliphatic index were reduced from 9.15 to 6.59 and from 76.49 to 69.52, respectively (15). Figure 2 shows the difference of solubility between (A) 60 µg/mL wild-type N^{pro} fusion (6H-N^{pro}-sGFPmut3.1) and (B) 120 µg/mL EDDIE fusion (6H-EDDIE-sGFPmut3.1), both under the same refolding conditions. It is obvious that the mutant showed tremendous improvement regarding solubility, thus leading to a much higher autoproteolytic activity and consequently higher product formation. One reason was the tendency of the wild-type N^{pro} to self-interact. This tendency was investigated by self-interaction blot analysis, in which

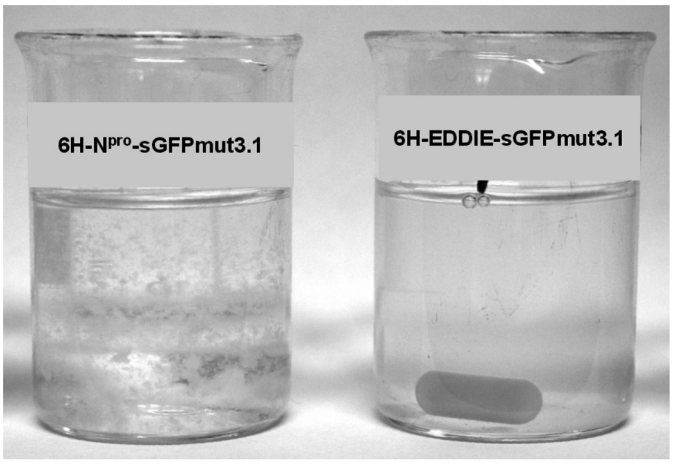

(A) (B)

FIG. 2. Solubility of Wild-type vs. Mutant EDDIE; (A) 60 µg/mL 6H-N^{pro}-sGFPmut3.1; (B) 120 µg/mL 6H-EDDIE-sGFPmut3.1; both in refolding buffer.

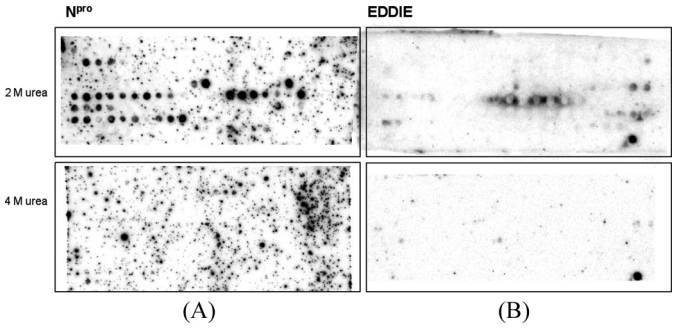

FIG. 3. Self-interaction Blots: cellulose membranes presenting synthetic overlapping 12mers of the entire amino acid sequence of wild-type N^{pro} (A) or mutant EDDIE (B) incubated with biotin-labeled N^{pro} (A) or biotin-labeled EDDIE (B) in the presence of 2 M (upper blots) or 4 M (lower blots) urea; black spot on right lower corner of EDDIE membranes = streptavidin-binding peptide (positive control).

cellulose membranes presenting synthetic overlapping peptides of the entire amino acid sequences of N^{pro} or EDDIE, respectively, were incubated with biotin-labeled N^{pro} or EDDIE. Binding to spots on the membrane was visualized by chemiluminescence (dark dots in Fig. 3). At 4 M urea, no interaction took place for either autoprotease. However, in the presence of 2 M urea, N^{pro} showed a strong tendency for self-interaction, corroborating the aggregation occurrence during refolding, at which point the urea concentration is even lower. As Fig. 3b shows, the mutant EDDIE was not affected.

Exchange of Critical Codons and Its Influence on Protein Homogeneity

After optimization of the amino acid sequence, expressed fusion proteins were investigated regarding their homogeneity. Analysis by 1D and 2D electrophoresis and of corresponding western blots showed that a major part of the existing microheterogeneity of expressed N^{pro} fusions results from the autoprotease, especially from the mutant EDDIE itself (data not shown). Dürrschmid et al. (31) showed that overexpression of recombinant proteins can reach levels higher than 30% of total cellular protein, which can put considerable stress on the host. The generated burden can influence the accuracy of protein translation. Factors such as mRNA stability and structure, target protein toxicity, proteolysis (2,32), and codon usage can play an important role (33) and are difficult to control during expression. Erroneous events during protein synthesis can be the result of missense errors or processing errors. Reports exist of rare codons, such as AGA or AGG, causing serious problems during protein synthesis (34,35). A so-called codon optimization can lead to a significant increase of heterologous protein expression (36,37).

As Fig. 4 shows, fusion proteins with the mutant EDDIE (lane 4) exhibited increased heterogeneity in

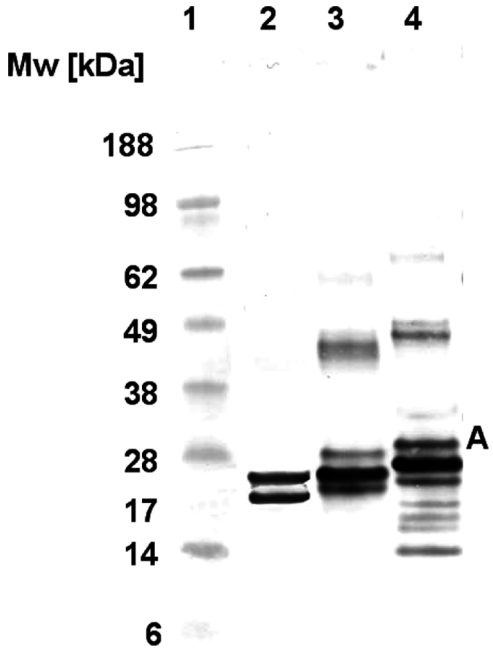

FIG. 4. Western Blot Against Npro: Molecular mass standard (lane 1), positive control, N^{pro} 100 ng (lane 2), IBs of N^{pro}-pep6His, 0.5 μg protein (lane 3), IBs of EDDIE-pep6His, 0.5 μg protein (lane 4).

molecular mass compared to the wild-type N^{pro}(lane 3), which indicated that the introduced mutations can be responsible for an increase in errors during protein translation. Therefore, EDDIE-pep6His was investigated concerning its homogeneity. Figure 4 shows MS analysis results for the elongated form (upper band marked with A). IBs of EDDIE-pep6His-UGA were solubilized and diluted into refolding buffer as described in the materials and methods section. After 24 hours, refolding and cleavage were completed. Samples were separated by RP-HPLC, and fractions were collected as numbered in Fig. 5a and analyzed by nanoESI Q-ToF MS. Figure 5a shows the chromatogram of the RP-HPLC separation and representative mass spectra of fractions 2 (Fig. 5b) and 5 (Fig. 5c), and Table 4 gives the complete results of the MS analysis. The results showed that the elongated form can be dedicated to overreading the stop codon UGA and should be prohibited by changing the stop codon to UAA. Analysis of various samples derived either from 2D gels or after RP-HPLC separation by mass spectrometry led to several possible codons that may be responsible for an enhanced erroneous protein expression of EDDIE compared to N^{pro}(Table 5). According to the data in Table 5, EDDIE-pep6His variants with improved codons were cloned, overexpressed in *E. coli*, and analyzed with SDS-PAGE and 2D-DIGE.

Figure 6 gives an impressive example, showing the effect of only one wrongly used codon on the quality of the recombinant protein. Figure 6a, lane 2, shows the original

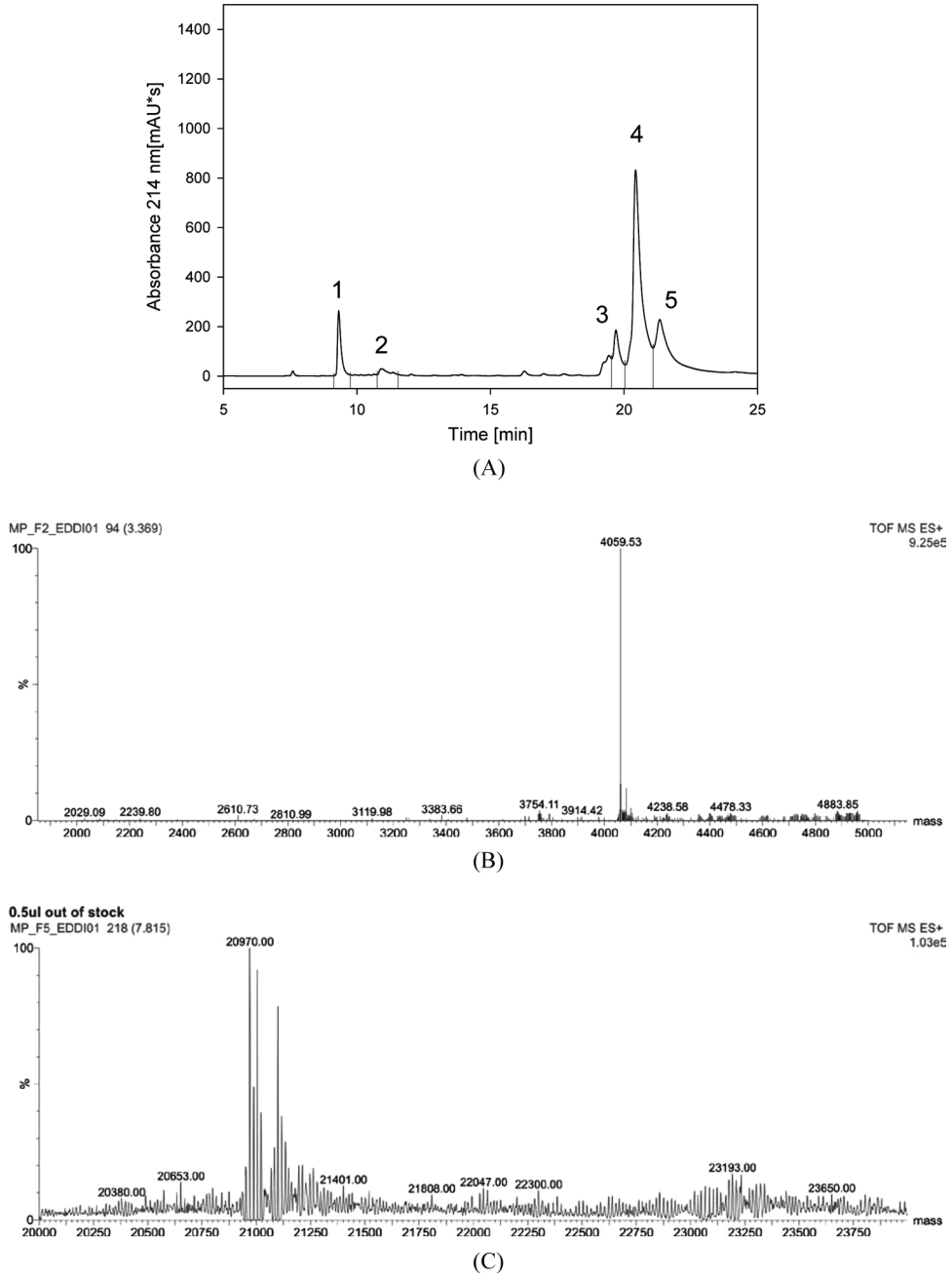

FIG. 5. Analysis by RP-HPLC and nanoESI Q-ToF MS to Clarify Reasons for Heterogeneity of EDDIE Fusions: (A) RP-HPLC chromatogram of separation of 0.4 mg/mL EDDIE-pep6His UGA after 24 hrs of refolding; the numbered fraction was analyzed by nanoESI Q-ToF MS. (B) Spectra after nanoESI Q-ToF MS of fractions 2 and 5 as numbered in (A); fraction 2 contains the cleaved prolonged peptide consisting of pep6His and the vector used with a corresponding mass of 4,059.53 Da; fraction 5 contains the overread of stop codon UGA/prolonged fusion protein EDDIE-pep6His + vector with the corresponding mass of 20,970.00 Da.

clone of EDDIE-pep6His (produced in HMS174), which contains an additional elongated isoform of the recombinant protein with a molecular mass of 23,194.0 Da. After a change of the stop codon UGA to UAA, the absence of this wrongly expressed protein was observed (Fig. 6, lanes 1 and 3). The improvement of homogeneity could also be confirmed by 2D DIGE analysis of these two EDDIE-pep6His variants because the elongated form could be detected only for EDDIE-pep6H is–UGA (green spots, Fig. 6b). Applying a semi-quantitative estimation of protein content on a 1D gel, the ratio of extended fusion protein could be determined as about 23% of the entire

TABLE 4
Results of nanoESI Q-ToF MS analysis of RP-HPLC separation of EDDIE-pep6His-UGA after a refolding duration of 24 hours

Fraction #	Expected content	Theoretical mass, Da	Measured mass, Da	Approved
1	pep6His peptide	1,838.9	1,839.11	YES
2	Elongated form due to overread of stop codon - pep6His + vector	4,059.06	4,059.53	YES
3	Cleaved EDDIE	19,149.5	19,150	YES
4	Cleaved EDDIE	19,149.5	19,150	YES
5	Uncleaved EDDIE-pep6His and elongated form	20,970.5/23,192	20,970/23,193	YES

expressed protein. Separation by 1D gel electrophoresis also showed that the additional exchange of codon 134 or 138 or both from GAG for GAA (lanes 4–6, Fig. 6) led to the expression of a number of truncated forms and an elongated form and did not lead to further improvement.

For all further described experiments, only EDDIE fusions with the optimized stop codon were used. These investigations were all carried out comparing one EDDIE-protein fusion, 6H-EDDIE-sGFPmut3.1, to one EDDIE-peptide fusion, EDDIE-pep6His, as an example because previous work has shown that a difference between these two categories of fusion protein is to be expected (15,23).

Dissolution Kinetics of IBs

For the characterization of the established N^{pro} fusion technology the basic steps of IB processing had to be investigated in more detail. Since the first crucial step of IB processing is the solubilization step, a method for determining dissolution kinetics of IBs had been established (20). Figure 7 shows examples demonstrating the determined dissolution kinetics for EDDIE-pep6His and EDDIE-sGFPmut3.1 in 4 M urea and 10 M urea (A, C) and 2 M and 5 M GuHCl (B, D). All experiments demonstrated the same tendencies: Only at the lowest concentration of 4 M urea and 2 M GuHCl could dissolution kinetics with significantly lower rate constants k_{sol} and yield be determined, and the yield was approximately half for experiments using 4 M urea vs. 2 M GuHCl. Second, the addition of the reducing agent MTG led to an increase of about 50% protein in solution for the lowest chaotrope concentrations. For chaotrope concentrations as high as 6 to 10 M urea or 3 to 5 M GuHCl, no significant difference in rate constant k_{sol} and yield could be determined. The higher the chaotrope concentration, the lower the influence of the reducing agent. Nevertheless, these findings were the same for EDDIE-pep6His and 6H-EDDIE-sGFPmut3.1,

TABLE 5
Codons that may cause errors during protein expression of EDDIE-pep6His in *E. coli*

Measured mass[a] [Da]	Possible codons responsible for errors during protein expression	Possible causes for erroneous fragments	Theoretical mass[b] [Da]	Amino acid exchange from N^{pro} to EDDIE	Codon exchanges to
15,680.0	GAG138	Ribosome stalling, ribosome drop off	15,680.4	YES	GAA138
15,969.0	GAG134	+1 frameshift until stop 1[c]	15,968.9	YES	GAA134
17,060.0	GAG134	+1 frameshift until stop 2[c]	17,061.2	YES	GAA134
15,732.0	ACC114	+1 frameshift until stop 2[c]	15,733.7	YES	–
17,403.0 17,402.0	ACC151	Ribosome stalling and/or ribosome drop off at R150	17,043.1	NO	–
23,194.0	STOP UGA	Read through until stop 2[c]	23,192.0	NO	STOP UAA

[a]Masses were measured with nanoESI Q-ToF MS.
[b]Theoretical masses were estimated with the Expasy ProtParam tool (http: //www.expasy.org/tools/protparam.html).
[c]Wrong stop codon, generated within the sequence because of a frameshift or read through of ribosomes.

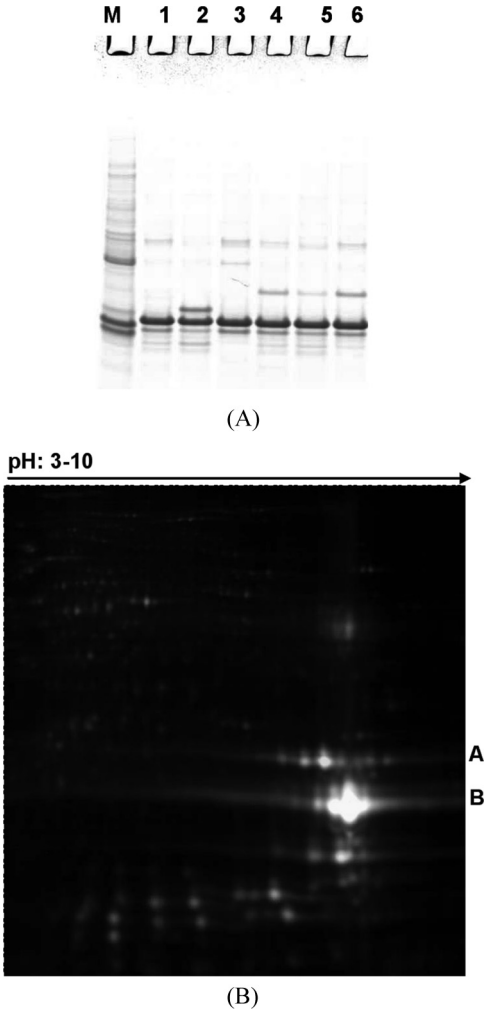

FIG. 6. Electrophoresis Showing Inclusion Bodies of EDDIE-pep6His Variants Prior to and After Codon Optimization of the Genetic Construct: (A) 1D gel, variants of EDDIE-pep6His (4–12%Bis-Tris NuPAGE®): M, molecular mass marker; lane 1, IBs of EDDIE-pep6HisUAA (HMS 174); lane 2, IBs of EDDIE-pep6His (HMS 174); lane 3, IBs of EDDIE-pep6HisUAA (BL21); lane 4, IBs of EDDIE-pep6His UAAGAA 134,138 (HMS 174); lane 5, IBs of EDDIE-pep6His UAAGAA 134 (HMS 174); lane 6, IBs of EDDIE-pep6His UAAGAA 138 (HMS 174). (B) 2D gel (12.5%AA), differential gel electrophoresis comparing EDDIE-pep6His-UGA (cy5, red) and EDDIE-pep6His-UAA (cy3, green); in yellow, proteins present in both clones at the same concentration.

except for the rate constants, which were half for the EDDIE-protein fusion compared to EDDIE-peptide fusion. These results demonstrate that the composition of the dissolution buffer can have a significant effect on the dissolution reaction with important consequences in the context of industrial production.

Refolding and Cleavage Kinetics

The next step of IB processing on the way to the functional protein/peptide usually is the refolding step. As described in the Introduction, common refolding reactions are aggregation limited and depend on the initial protein concentration. Equation (1) by Kiefhaber et al. (22) expresses this relationship. In the case of N^{pro} technology, the autoprotease must refold to regain its functionality, cleave itself at its C terminus, and release the target, which in case of a protein again must refold to regain its functionality. Therefore, within this "refolding" step for EDDIE-peptide fusion, at least two kinetic steps take place: refolding of the autoprotease and cleavage. On this basis, the amount of cleaved autoprotease and/or peptide can be determined by RP-HPLC analysis, and the calculated kinetics should include refolding of the autoprotease and the cleavage process. Concerning 6H-EDDIE-sGFPmut3.1, additional refolding of green fluorescent protein (GFP) had to take place, detectable by increased fluorescence. The determined kinetics therefore includes not only refolding and cleavage of the autoprotease but also of GFP. Figure 8 shows representative kinetics of increasing concentration of EDDIE-pep6His (A) and 6H-EDDIE-sGFPmut3.1 (B) (23). The determined kinetics of 6H-EDDIE-sGFPmut3.1 conformed to Eq. (1) and showed decreasing yield with increasing initial protein concentration (Fig. 8b). In contrast, the kinetics determined for EDDIE-pep6His showed a constant cleavage yield across a wide range of protein concentrations with a decreasing rate constant (Fig. 8a), which did not conform to Equation (1).

Therefore, Kaar et al. (23) established a model including a side reaction of misfolding following a first-order kinetics, in which the overall yield Y(t) can be expressed independently from protein concentration as:

$$Y(t) = \frac{k_1}{k_1 + k_2} - \frac{k_1}{k_1 + k_2} e^{-(k_1+k_2)t} \qquad (2)$$

with k_1 [s^{-1}] the overall rate constant of folding and cleavage, k_2 [s^{-1}] the overall rate constant of misfolding, and t [s] the time (23). As also shown by Kaar et al. (23), this phenomenon is not confined to EDDIE-pep6His but could be determined for a number of other EDDIE-peptide fusions, as well. A great deal of effort has been put into explaining this different kinetics for EDDIE-peptide fusions. Ueberbacher et al. (38) demonstrated that the decrease in rate constants with increasing initial protein concentration was dominantly caused by a parallel increase in chaotrope concentration, primarily because the required protein concentration for refolding processes was adjusted by simply diluting IB solutions into refolding buffer. Because the IB solution contained a high chaotrope concentration, the concentration of this compound also increased with increasing protein concentration. Adjusting the same chaotrope concentration for increasing protein concentration led to the rate constants becoming constant.

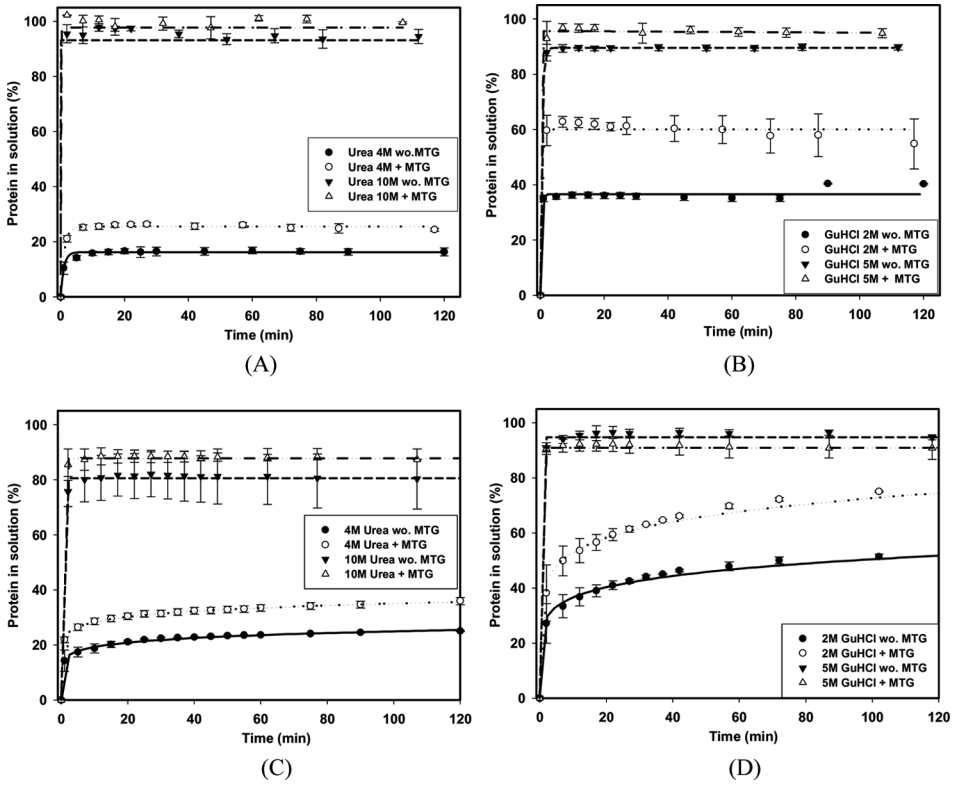

FIG. 7. Dissolution Kinetics of EDDIE-pep6His (A, B) and 6H-EDDIE-sGFPmut3.1 (C, D) in 4 M and 10 M Urea ±100 mM MTG (A, C) and 2 M and 5 M GuHCl ± 100 mM MTG (B, D).

Figure 9 shows the refolding and cleavage kinetics of increasing concentrations of EDDIE-K-pep6His (same amino acid as pep6His with an additional lysine at the N terminus) in the presence of increasing urea, as adjusted by dilution of IB solutions into refolding buffer (Fig. 9a). In comparison, Fig. 9b shows the refolding and cleavage kinetics of increasing concentrations of this fusion protein in the presence of constant urea. With adjustment of the same chaotrope concentration for increasing protein concentration, the rate constants became almost constant (Fig. 9c). In addition, this kinetics was shown, since the fusion protein used differs only in one amino acid (an additional lysine on the N terminus of the target) from EDDIE-pep6His. A comparison of the kinetics shown in Fig. 9a to the kinetics of EDDIE-pep6his shown in Fig. 8a demonstrates the strong influence on the determined kinetics of the first amino acid of the target protein/peptide: The introduction of lysine on the N terminus led to a 5-fold decrease of k_1(38). Achmüller et al. (15) had already described this strong influence of the first amino acid, showing that an N-terminal proline fully inhibited autoproteolytic cleavage.

ATR-FTIR and fluorescence measurements showed that the 3D structure of the autoprotease was already largely built at the start of refolding/cleavage kinetics; no significant structural change could be determined during this time span. Turbidity measurements were carried out to investigate aggregation behavior during the refolding/cleavage of EDDIE-peptide fusions. It could be demonstrated that low aggregation occurred in parallel or even after cleavage had taken place, probably caused by self aggregation of the cleaved autoproteases (38). In summary, the determined kinetics of EDDIE-peptide fusions are not aggregation limited and were dominated by the cleavage kinetics because refolding of the autoprotease was finalized beforehand. The dominance of cleavage on the determined kinetics was further corroborated by the strong influence of the first amino acid of the target protein/peptide on the determined cleavage kinetics. The rate constant of cleavage increases up to 9-fold with the exchange of the first amino acid from lysine to either serine or cysteine (38).

Interaction Between Dissolution Condition and Refolding and Cleavage Kinetics

Singh and Panda (39) stated that the type and concentration of chaotrope used for dissolution of IBs affects refolding behavior and protein yield. It was assumed that mild solubilization of IB proteins without generating the random coil in which hydrophobic patches are not fully exposed would improve renaturation of proteins from IBs.

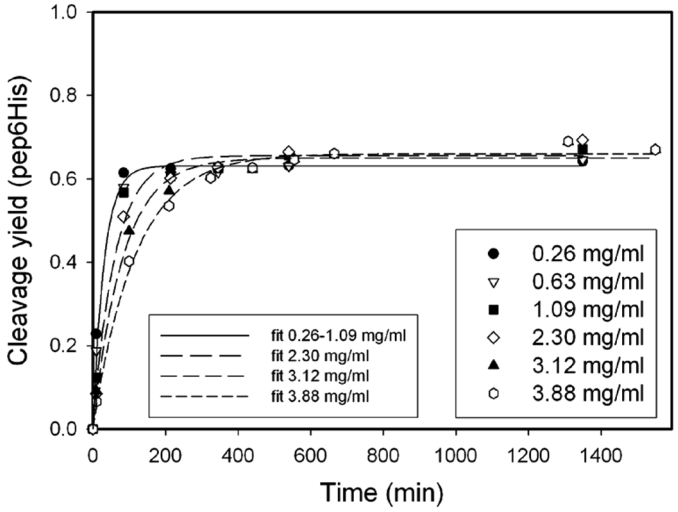

(A)

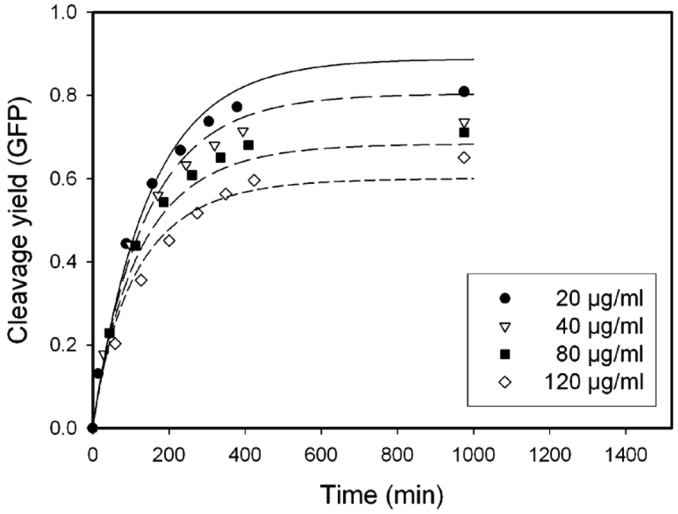

(B)

FIG. 8. Refolding and Cleavage Kinetics of EDDIE-pep6His (A) and 6H-EDDIE-sGFPmut3.1 (B): lines represent fits to Eq. (2) for EDDIE-pep6His and fits to Equation (1) for 6H-EDDIE-sGFPmut3.1. From ref (17). with permission.

Because we have already shown that except for very low chaotrope concentration, solubilization of IBs is comparable for 6 to 10 M urea and 3 to 5 M GuHCl, it was of high interest whether the kind and concentration of chaotrope used for dissolution would change the determined refolding and cleavage kinetics. Therefore, IBs of EDDIE-pep6His and 6H-sGFPmut3.1 were dissolved in increasing concentrations of urea (4, 6, 8, or 10 M) and GuHCl (2, 3, 4, or 5 M) with and without MTG, and refolding/cleavage kinetics were determined as described earlier. The design differed in that for all corresponding experiments, the protein concentration was adjusted to 0.4 mg/mL initial protein and the chaotrope

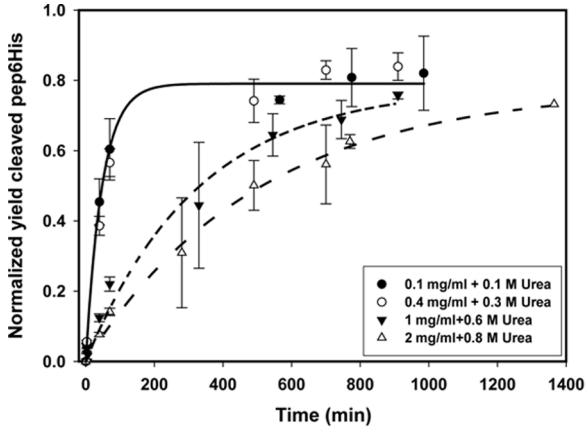

(A)

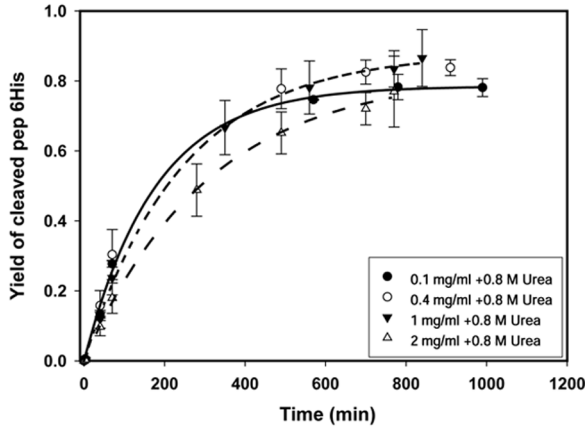

(B)

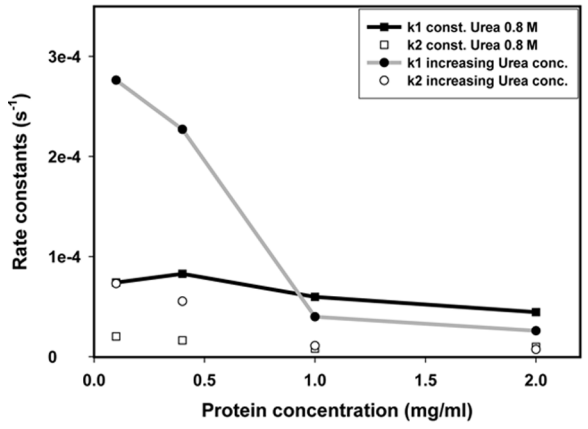

(C)

FIG. 9. Influence of Urea and First Amino Acid of Target on Refolding and Cleavage of EDDIE-K-pep6His: refolding and cleavage kinetics of EDDIE-K-pep6His in the presence of increasing concentrations of urea (A), in the presence of a constant concentration of urea (B), and k_1 and k_2 for kinetics shown in (A) and (B) calculated with Eq. (2) (C). Figure 9a is from ref (28). with permission.

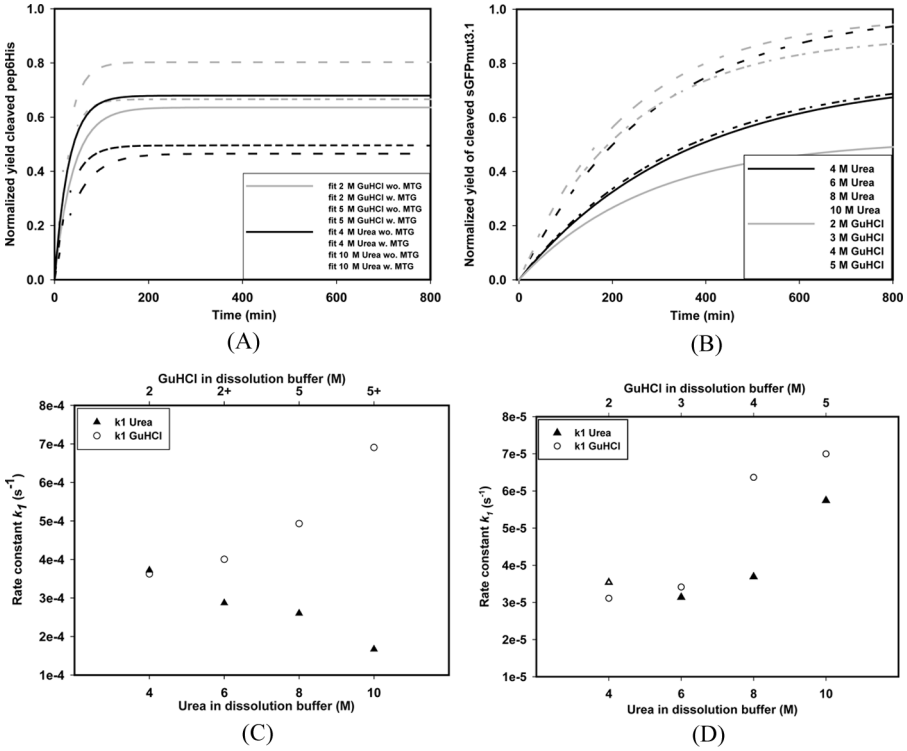

FIG. 10. Influence of Dissolution Conditions on Refolding and Cleavage Kinetics: refolding and cleavage kinetics of EDDIE-pep6His (A) and 6H-EDDIE-sGFPmut3.1 (B) after dissolution of IBs in increasing concentrations of urea or GuHCl. Corresponding rate constants k_1 calculated by Eq. (2) for EDDIE-pep6His (C) and calculated by Eq. (1) for 6H-EDDIE-GFPmut3.1 (D); conditions during refolding were the same for corresponding kinetics independent of prior dissolution condition.

concentration was the same regardless of the concentration previously used for dissolution. Thus, the conditions during refolding were constant for all corresponding experiments, with only the conditions for dissolution differing. The determined kinetics were fit to either Eq. (1) for 6H-EDDIE-sGFPmut3.1 or Eq. (2) for EDDIE-pep6His, and the calculated rate constants k_1 are shown in Fig. 10. First, as shown before, the rate constants of EDDIE-pep6His were generally one order of magnitude faster than those of 6H-EDDIE-sGFPmut3.1. Second, it was obvious that the type and concentration of chaotrope used for dissolution clearly influenced the determined kinetics, even though the effect was diverse. The rate constants of refolding/cleavage k_1 determined for 6H-sGFPmut3.1 increased with an increase of either chaotrope. Comparing the lowest to the highest concentration of chaotrope, the rate constant was more than 2-fold greater in case of GuHCl (Fig. 10d). For EDDIE-pep6His, the increase of rate constant k_1 was also 2-fold higher using 2.5-fold of GuHCl for dissolution, while the rate constant determined for refolding/cleavage after dissolution in urea decreased with increasing urea concentration (Fig. 10c). Concerning the yield of cleaved target, usage of 10 M urea or 4 M or 5 M GuHCl led to a yield of cleaved and functional GFP of more than 80%, while all other chaotrope concentrations showed a lower yield of a minimum 40% (Figs. 10a and b).

CONCLUSION

This work provides an overview of the basis of development and application of N^{pro} autoprotease fusion technology. N^{pro} fusion technology has proved to be a versatile tool for high-yield overexpression of proteins and peptides in *E. coli*. The core of the system is the autoproteolytic activity of N^{pro} upon renaturation that leads to a product with an authentic N terminus as well as the remarkably high fermentation titers that can be achieved for many proteins, in particular oligopeptides. Along with engineering the amino acid sequence and the genetic construct, a variety of technologies have been established to build a generic production platform. The knowledge of the kinetics of dissolution of IBs and the autoproteolytic reaction allows proper design and modeling of the production process.

For future perspectives, it should be noted that experiments have been carried out using N^{pro} technology for column processes, in which refolding and cleavage are performed on chromatographic resins. Loading of 50 mg/mL and a final refolding concentration up to 15 mg/mL

with cleavage yields of 60% are very promising and will further increase productivity of N^{pro} technology (40).

ACKNOWLEDGEMENTS

This work was carried out at the Austrian Center of Biopharmaceutical Technology (ACBT), which is a Competence Center within the K_{ind}-K_{net} program funded by the Austrian Federal Ministry of Economics and Labor and the provinces Vienna and Tyrol. Mass spectrometric analysis was done by D.I. Stadlmann Johannes from the Department of Chemistry, University of Life Science and Natural Resources, Vienna, Austria.

REFERENCES

1. Research, B. (2008) Protein Drugs: Global Markets and Manufacturing Technologies (BIO021C).
2. Hannig, G.; Makrides, S.C. (1998) Strategies for optimizing heterologous protein expression in Escherichia coli. *Trends Biotechnol.*, 16 (2): 54–60.
3. Stevens, R.C. (2000) Design of high-throughput methods of protein production for structural biology. *Structure*, 8 (9): 177–185.
4. Hirel, P.H.; Schmitter, J.M.; Dessen, P.; Fayat, G.; Blanquet, S. (1989) Extent of N-terminal methionine excision from Escherichia coli proteins is governed by the side-chain length of the penultimate amino acid. *Proc. Nat. Acad. Sci. USA*, 86 (21): 8247–8251.
5. Boix, E.; Wu, Y.; Vasandani, V.M.; Saxena, S.K.; Ardelt, W.; Ladner, J.; Youle, R.J. (1996) Role of the N terminus in RNase a homologues: Differences in catalytic activity, ribonuclease inhibitor interaction and cytotoxicity. *J. Mol. Biol.*, 257 (5): 992–1007.
6. Endo, S.; Yamamoto, Y.; Sugawara, T.; Nishimura, O.; Fujino, M. (2001) The additional methionine residue at the N-terminus of bacterially expressed human interleukin-2 affects the interaction between the N- and C-termini. *Biochemistry*, 40 (4): 914–919.
7. Nilsson, J.; Stahl, S.; Lundeberg, J.; Uhlen, M.; Nygren, P. (1997) Affinity fusion strategies for detection, purification, and immobilization of recombinant proteins. *Protein Expr. Purif.*, 11 (1): 1–16.
8. Chong, S.; Montello, G.E.; Zhang, A.; Cantor, E.J.; Liao, W.; Xu, M.Q.; Benner, J. (1998) Utilizing the C-terminal cleavage activity of a protein splicing element to purify recombinant proteins in a single chromatographic step. *Nucl. Acids Res.*, 26 (22): 5109–5115.
9. Paulus, H. (2000) Protein splicing and related forms of protein autoprocessing. *Annu. Rev. Biochem.*, 69 (1): 447–496.
10. Mills, K.V.; Dorval, D.M.; Lewandowski, K.T.; Mills, K.V. (2005) Kinetic analysis of the individual steps of protein splicing for the Pyrococcus abyssi polII intein. *J. Biol. Chem.*, 280 (4): 2714–2720.
11. Perler, F.B.; Adam, E. (2000) Protein splicing and its applications. *Curr. Opin. Biotechnol.*, 11 (4): 377–383.
12. Perler, F.B.; Davis, E.O.; Dean, G.E.; Gimble, F.S.; Jack, W.E.; Neff, N.; Noren, C.J.; Thorner, J.; Belfort, M. (1994) Protein splicing elements: inteins and exteins–a definition of terms and recommended nomenclature. *Nucl. Acids Res.*, 22 (7): 1125–1127.
13. Chong, S.; Mersha, F.B.; Comb, D.G.; Scott, M.E.; Landry, D.; Vence, L.M.; Perler, F.B.; Benner, J.; Kucera, R.B.; Hirvonen, C.A. (1997) Single-column purification of free recombinant proteins using a self-cleavable affinity tag derived from a protein splicing element. *Gene*, 192 (2): 271–281.
14. Lishi, W.; Jung Hye, K.; Ki Hyung, K.; Lee, E.K. (2010) Expression of intein-tagged fusion protein and its applications in downstream processing. *J. Chem. Technol. Biot.*, 85 (1): 11–18.
15. Achmüller, C.; Kaar, W.; Ahrer, K.; Wechner, P.; Hahn, R.; Werther, F.; Schmidinger, H.; Cserjan-Puschmann, M.; Clementschitsch, F.; Striedner, G. (2007) N^{pro} fusion technology to produce proteins with authentic N termini in E.coli. *Nature Methods*, 4 (12): 1037–1043.
16. Rümenapf, T.; Stark, R.; Heimann, M.; Thiel, H.J. (1998) N-terminal protease of pestiviruses: Identification of putative catalytic residues by site-directed mutagenesis. *J. Virol.*, 72 (3): 2544–2547.
17. Stark, R.; Meyers, G.; Rümenapf, T.; Thiel, H.J. (1993) Processing of pestivirus polyprotein: Cleavage site between autoprotease and nucleocapsid protein of classical swine fever virus. *J. Virol.*, 67 (12): 7088–7095.
18. Georgiou, G.; Valax, P. (1999) [3] Isolating inclusion bodies from bacteria. *Method. Enzymol.*, 309: 48–58.
19. Jungbauer, A.; Kaar, W. (2007) Current status of technical protein refolding. *J. Biotechnol.*, 128 (3): 587–596.
20. Dürauer, A.; Mayer, S.; Sprinzl, W.; Jungbauer, A.; Hahn, R. (2009) High througput system for determining dissolution kinetics of inclusion bodies. *Biotechnol. J.*, 4 (5): 722–729.
21. Zettlmeissl, G.; Rudolph, R.; Jaenicke, R. (1979) Reconstitution of lactic dehydrogenase. Noncovalent aggregation vs. reactivation. 1. Physical properties and kinetics of aggregation. *Biochemistry*, 18 (25): 5567–5571.
22. Kiefhaber, T.; Rudolph, R.; Kohler, H.H.; Buchner, J. (1991) Protein aggregation in vitro and in vivo: A quantitative model of the kinetic competition between folding and aggregation. *Biotechnology*, 9 (9): 825–829.
23. Kaar, W.; Ahrer, K.; Dürauer, A.; Greinstetter, S.; Sprinzl, W.; Wechner, P.; Clementschitsch, F.; Bayer, K.; Achmüller, C.; Auer, B. (2009) Refolding of Npro fusion proteins. *Biotechnol. Bioeng.*, 104 (4): 774–784.
24. Clementschitsch, F.; Kern, J.; Florentina, P.; Karl, B. (2005) Sensor combination and chemometric modelling for improved process monitoring in recombinant E. coli fed-batch cultivations. *J. Biotechnol.*, 120 (2): 183–196.
25. Frank, R.; Overwin, H. (1996) SPOT synthesis. Epitope analysis with arrays of synthetic peptides prepared on cellulose membranes. *Method Mol. Biol.*, 66: 149–169.
26. Pflegerl, K.; Hahn, R.; Berger, E.; Jungbauer, A. (2002) Mutational analysis of a blood coagulation factor VIII-binding peptide. *J. Pept. Res.*, 59 (4): 174–182.
27. Hartl, M.; Reiter, F.; Bader, A.G.; Castellazzi, M.; Bister, K. (2001) JAC, a direct target of oncogenic transcription factor Jun, is involved in cell transformation and tumorigenesis. *Proc. Nat. Acad. Sci. USA*, 98 (24): 13601–13606.
28. Cui, C.; Zhao, W.; Chen, J.; Wang, J.; Li, Q. (2006) Elimination of in vivo cleavage between target protein and intein in the intein-mediated protein purification systems. *Protein Expr. Purif.*, 50 (1): 74–81.
29. Király, O.; Guan, L.; Szepessy, E.; Tóth, M.; Kukor, Z.; Sahin-Tóth, M. (2006) Expression of human cationic trypsinogen with an authentic N terminus using intein-mediated splicing in aminopeptidase P (pepP) deficient Escherichia coli. *Protein Expr. Purif.*, 48 (1): 104–111.
30. Srinivasa Babu, K.; Muthukumaran, T.; Antony, A.; Prem Singh Samuel, S.D.; Balamurali, M.; Murugan, V.; Meenakshisundaram, S. (2009) Single step intein-mediated purification of hGMCSF expressed in salt-inducible E. coli. *Biotechnol. Lett.*, 31 (5): 659–664.
31. Dürrschmid, K.; Marzban, G.; Dürrschmid, E.; Striedner, G.; Clementschitsch, F.; Cserjan-Puschmann, M.; Bayer, K. (2003) Monitoring of protein profiles for the optimization of recombinant fermentation processes using public domain databases. *Electrophoresis*, 24 (1–2): 303–310.
32. Baneyx, F. (1999) Recombinant protein expression in Escherichia coli. *Curr. Opin. Biotechnol.*, 10 (5): 411–421.
33. Jana, S.; Deb, J.K. (2005) Strategies for efficient production of heterologous proteins in Escherichia coli. *Appl. Microbiol. Biot.*, 67 (3): 289–298.

34. Dong, H.; Nilsson, L.; Kurland, C.G. (1996) Co-variation of tRNA abundance and codon usage in Escherichia coli at different growth rates. *J. Mol. Biol.*, 260 (5): 649–663.
35. Sorensen, H.P.; Sperling-Petersen, H.U.; Mortensen, K.K. (2003) Production of recombinant thermostable proteins expressed in Escherichia coli: completion of protein synthesis is the bottleneck. *J. Chromatogr. B*, 768: 207–214.
36. Lakey, D.L.; Voladri, R.K.R.; Edwards, K.M.; Hager, C.; Samten, B.; Wallis, R.S.; Barnes, P.F.; Kernodle, D.S. (2000) Enhanced production of recombinant Mycobacterium tuberculosis antigens in Escherichia coli by replacement of low-usage codons. *Infect. Immun.*, 68 (1): 233–238.
37. Zhou, Z.; Schnake, P.; Xiao, L.; Lal, A.A. (2004) Enhanced expression of a recombinant malaria candidate vaccine in Escherichia coli by codon optimization. *Protein Expr. Purif.*, 34 (1): 87–94.
38. Ueberbacher, R.; Dürauer, A.; Ahrer, K.; Mayer, S.; Sprinzl, W.; Jungbauer, A.; Hahn, R. (2009) EDDIE fusion proteins: Triggering autoproteolytic cleavage. *Process Biochem.*, 44 (11): 1217–1224.
39. Singh, S.M.; Panda, A.K. (2005) Solubilization and refolding of bacterial inclusion body proteins. *J. Biosci. Bioeng.*, 99 (4): 303–310.
40. Schmoeger, E.; Berger, E.; Trefilov, A.; Jungbauer, A.; Hahn, R. (2009) Matrix-assisted refolding of autoprotease fusion proteins on an ion exchange column. *J. Chromatogr. A*, 1216 (48): 8460–8469.